

Improvement of nuclear reaction modeling for the production of ^{47}Sc on natural vanadium targets for medical applications

Alessandro Colombi^{1,2*}, Francesca Barbaro^{3,1}, Luciano Canton³, Mario Pietro Carante^{1,2}, and Andrea Fontana²

¹Università di Pavia – Dipartimento di Fisica, via A. Bassi 6, 27100 Pavia, Italy

²INFN - Sezione di Pavia, via A. Bassi 6, 27100 Pavia, Italy

³INFN - Sezione di Padova, via F. Marzolo 8, 35131 Padova, Italy

Abstract. The proton-induced reaction on natural vanadium targets is studied for the production of the innovative theranostic radionuclide ^{47}Sc as well as of its contaminants, mainly ^{46}Sc . The theoretical excitation functions are calculated using the nuclear reaction code TALYS and are compared with the most recent experimental data. A better agreement between the theoretical curves and the data is achieved with an optimization of the nuclear level density parameters. The obtained improvements represent a useful and important result for accurate evaluations of yields and purities which are needed quantities for subsequent dosimetric studies, in view of the radiopharmaceutical applications of ^{47}Sc . The optimization procedure is explained and shown for ^{47}Sc and ^{46}Sc , and also a comparison among the theoretical and experimental cumulatives is given (for the main contaminant) in addition to an estimation of the production yields for two irradiation conditions for both nuclides.

1 Introduction

In the last few years the production of theranostic radionuclides has gained an increasing interest of the scientific community for their important applications in nuclear medicine. In particular ^{47}Sc represents, at the moment, one the most promising radionuclides to be studied [1, 2] due to its interesting decay characteristics ($T_{1/2}=3.35$ d, $E_{\gamma}=159$ keV, $I_{\gamma}=68.4\%$, $E_{\beta^-}=162$ keV) [3] which, on one side, make it suitable to study the slow biodistribution of large molecules and to perform SPECT (Single Photon Emission Computed Tomography) imaging, and on the other side to treat small size tumours thanks to the high intensity β^- decay. Furthermore, the combination of ^{47}Sc with other Sc-isotopes as ^{43}Sc or ^{44}Sc , which are positron emitters, is very interesting for the possibility to integrate the diagnostic PET (Positron Emission Tomography) studies [2, 4] to the therapeutic applications of ^{47}Sc .

* Corresponding author: alessandro.colombi@pv.infn.it

In this field, nuclear physics studies play a great role especially to select interesting production routes and the most promising conditions to produce the nuclide of interest with sufficiently high yield and purity for its nuclear medicine applications [5]. Indeed, particular emphasis is devoted to the evaluation of the main contaminants, mainly ^{46}Sc ($T_{1/2} = 83.79$ d), which can affect the final purity and contribute to the final dose imparted to the patients. At the moment all the possible reaction routes are investigated to produce ^{47}Sc with both accelerators and nuclear reactors. In particular, this work is focused on proton-induced nuclear reactions using natural vanadium targets, which have been studied within the PASTA project (Production with Accelerators of Sc-47 for Theranostic Applications) in the framework of LARAMED (LABoratory of RADioisotopes for MEDicine) program at INFNLegnaro National Laboratories (INFN-LNL), with the final goal to produce the nuclide of interest by using the INFN-LNL 70 MeV proton cyclotron. Nevertheless, at the moment, also other reactions are under study using titanium targets [6].

As described in Ref. [7], for the $^{\text{nat}}\text{V}(p, x)^{47}\text{Sc}$ reaction the theoretical excitation functions, calculated using the nuclear reaction code TALYS [8], are not in agreement with the available experimental data, representing a problem in the evaluation of ^{47}Sc and of its contaminants in view of the theranostic applications. Therefore, in this work our aim is to find a better description of the cross sections investigating the most recent microscopic models implemented inside the TALYS code. Our attention is focused on the nuclear level density parameters to reproduce especially the cross sections of ^{47}Sc and ^{46}Sc , and also the cross sections of all the other nuclides studied in the project (^{43}Sc , ^{44g}Sc , ^{44m}Sc , ^{48}Sc , ^{42}K , ^{43}K , ^{48}V , ^{48}Cr , ^{49}Cr , ^{51}Cr).

2 Nuclear reaction modeling

In the field of radiopharmaceutical production, the use of nuclear reaction codes is essential to model a nuclear reaction and to estimate the yields of the nuclide of interest as well as of the contaminants, starting from the studies of the cross sections. Nuclear reactions are very complex to analyze since several aspects have to be taken into account, as the co-existence of the different reaction mechanisms, like the compound nucleus formation and evaporation, the preequilibrium process and the direct reaction mechanism. Among the available nuclear reaction codes, the TALYS simulation package (v. 1.9) [8] has been considered in this work for the theoretical analyses of the cross sections for the $^{\text{nat}}\text{V}(p, x)^{47}\text{Sc}$ reaction. The code is very versatile and a variety of different models are implemented in for the description of the processes in the interaction between a projectile and a target, going from phenomenological models to modern microscopic approaches. In particular, inside the code, there are four models for the preequilibrium emission and six models for the description of the nuclear level density, resulting therefore in several combinations of models that can be considered for any reaction. Different possibilities can be examined but in literature many calculations refer to the use of two specific combinations of models: the so-called “TALYS default” (based on the default options of the code) and “TALYS adjusted” [10] (based on another configuration usually used to replace the default one). None of the options is in some cases either the best choice or the unique possibility and therefore alternatives can be also investigated. As described in Ref. [11], a possibility is given by considering all the combinations of models and using descriptive statistical quantities, mainly quartiles. With this approach, instead of plotting all the curves, only a statistical band is constructed from the interquartile range, given by the difference between the third (Q3) and the first (Q1) quartiles. Starting from the band, for each energy a theoretical reference curve (BTE which stands for “Best Theoretical

Evaluation”) can be introduced as the centroid of the band, to which an uncertainty (given by the half-width of the band) is associated:

$$\sigma_{BTE} = \frac{Q_1 + Q_3}{2} \quad \Delta_{BTE} = \frac{Q_3 - Q_1}{2}. \quad (1)$$

The new curve together with the corresponding uncertainty can be used for the further estimations of yields and purities of the produced nuclides. Nevertheless, another possible choice can be represented by the improvements on a specific model, which is the approach used in this work to better reproduce the trend of the experimental data. The used procedure is not a pure theoretical approach but more likely can be described as a phenomenological one, trying to use already developed models and adjust some of their parameters to obtain new curves to reproduce the data, in view of the practical applications of the produced radionuclides. In particular the attention has been addressed to the three microscopic models for the level densities, which are based on Hartree-Fock Methods (HFM), comprehensive of HF plus Bardeen-Cooper-Schrieffer (HF-BCS) [12] and HF Bogoliubov (HFB) [13, 14]. Inside TALYS the HFM level densities are tabulated for different energy values and subsequently are rescaled according to the following transformation:

$$\rho(E, J, \pi) = \exp(c\sqrt{E-p}) \rho_{HFM}(E-p, J, \pi) \quad (2)$$

which depends on the two parameters c and p . The former acts as an overall normalization while the latter could represent an energy shift caused by pairing or even shell effects. Inside the code each microscopic model has tables of parameters that allow to obtain new level densities starting from the pure theoretical HFM ones. Nevertheless, the curves of the microscopic models, with their tabulated values of the parameters, do not always describe well the cross sections of a given reaction, but the possibility to vary the parameters is given, as stated in the TALYS manual [15] as well as in the RIPL library [16].

In this work a combination of models has been considered: for the nucleon-nucleus interaction the so-called JLM (Jeukenne-Lejeune-Mahaux) semi-microscopic optical potential model [17, 18], while for the preequilibrium process the default option, based on the exciton model with transition rates calculated numerically. Regarding the nuclear level density, a tuning of the two parameters has been performed considering the model based on HF-BCS method that is denoted inside the code with the keyword *ldmodel 4*, in order to obtain a better agreement between the theoretical curves and the experimental data for all the nuclides studied in the PASTA project. Specifically, an initial grid search has been performed on the two parameters considering all the nuclides involved and an initial set of values has been obtained by a qualitative agreement, based on a visual analysis, between the TALYS curves and the data. As a second step a MINUIT [19] global chi-square minimization procedure, using the combination of gradient and simplex optimizations, has been implemented to refine the solutions, arriving to the final optimal set used to obtain new theoretical curves which are referred to as “TALYS modified”. The final set reported in Tab. 1 is not intended as the unique possible solution, since other possibilities could also be explored with different parameters. Nevertheless, with the found solution a very high accuracy in the description of the cross sections has been achieved, especially for the main contaminant.

Table 1. Final set of values of the level density parameters.

	^{42}K	^{43}K	^{44}Sc	^{46}Sc	^{48}Sc	^{48}V	^{48}Cr
c	1.27443	1.09559	1.97876	0.339592	-	-	0.234421
p	-	0.140468	1.11855	-1.17731	0.449064	-0.25841	-

3 Results and discussion

The reaction with protons on natural vanadium targets has been considered, within the energy range 26-70 MeV, for the production of ^{47}Sc , ^{43}Sc , ^{44g}Sc , ^{44m}Sc , ^{46}Sc , ^{48}Sc , ^{42}K , ^{43}K , ^{48}V , ^{48}Cr , ^{49}Cr , ^{51}Cr . A complete discussion of all the nuclides studied in the PASTA project is given in [9], while in this paper only the ^{47}Sc and ^{46}Sc cases are shown with BTE and TALYS modified approaches. In the following figures the comparison between the theoretical cross

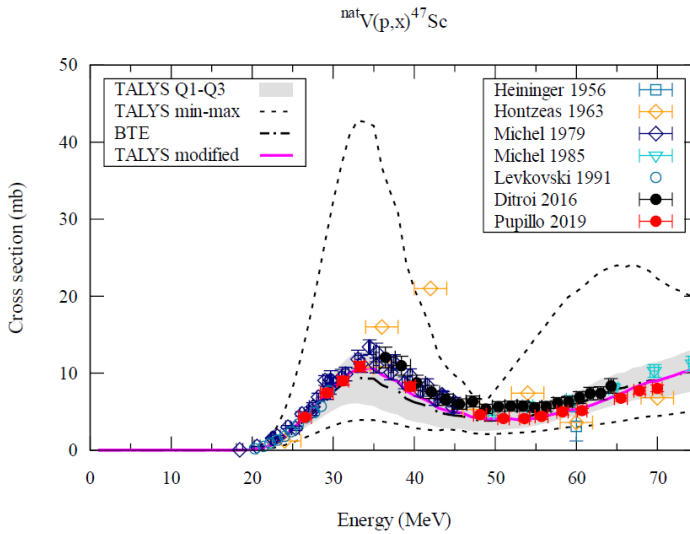


Fig. 1. Cross section for the $^{nat}\text{V}(p,x)^{47}\text{Sc}$ with the BTE approach and with TALYS modified.

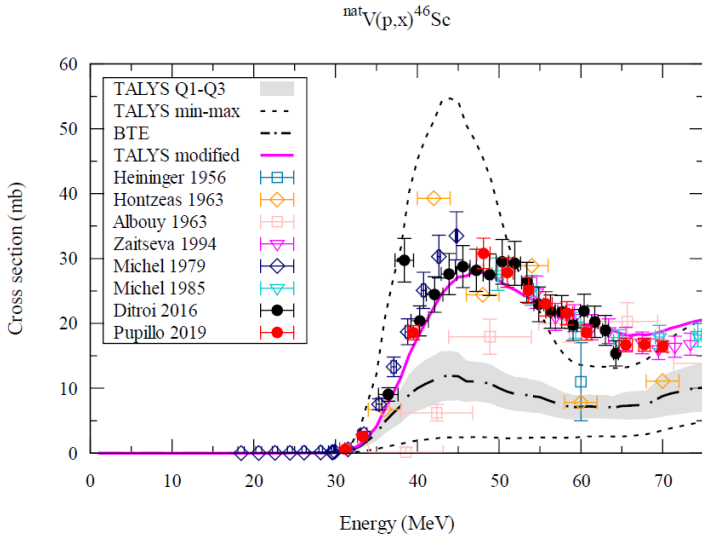


Fig. 2. Cross section for the ${}^{\text{nat}}V(p,x){}^{46}\text{Sc}$ with the BTE approach and with TALYS modified.

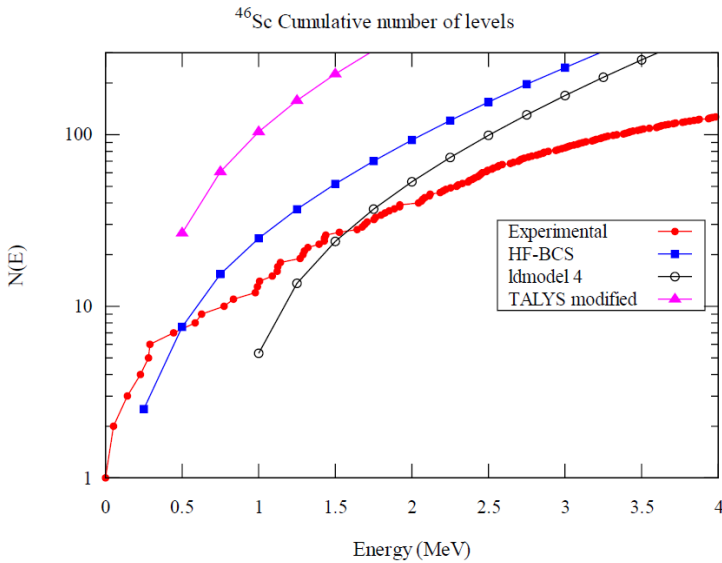


Fig. 3. Comparison among theoretical and experimental cumulatives.

sections and the experimental data [7, 20-27] and the comparison among the cumulatives (only for ${}^{46}\text{Sc}$) are shown.

In Figs. 1 and 2 all the models are represented with the statistical representation described in the previous section. The dashed lines correspond to the minimum and maximum among the combinations, the shaded area is the interquartile range, containing the 50% of the models, while the dash-dot line is the BTE curve (the central curve of the band). In Fig. 1 the trend of the recent data is quite well described by the BTE curve, while in Fig. 2 the statistical

approach allows to observe that 50% of the models does not reproduce the trend of the recent data not only in the region around the cross section peak but also in the area of high energy (60-70 MeV), where the TALYS models show a different behavior if compared to the one of the data. Instead of the BTE curve, a better description is given by the solid line, TALYS modified, which is the curve obtained with the tuning procedure of the nuclear level density parameters. In this case the curves for both ^{47}Sc and ^{46}Sc well reproduce the trend of the recent data in all the energy regions resulting in more accurate estimations of their production yields and therefore also of the radionuclidic purity of the nuclide of interest.

In Fig. 3 the comparison among the experimental cumulative, represented with points, and three theoretical cumulatives is shown, as an example, only for ^{46}Sc . The one represented with squares corresponds to the curve obtained with the HF-BCS method (whose values are tabulated inside the code) for which both the c and p parameters are equal to zero. The cumulative with open circles is the one of the model indicated with *ldmodel 4* which is derived from the HF-BCS cumulative using the tables of the parameters inside the code. The last cumulative with triangles is obtained with the new values of c and p found in this work. From the figure a disagreement between the TALYS modified curve with the experimental one is evident, but also the other two theoretical cumulatives do not provide an accurate description. This behavior could be explained by considering that the models, available at the moment, do not take into account all the possible phenomenological effects and significant contributions, as the isospin dependence in statistical processes (as already stated in the literature [28]). This may underline the need of the optimizations to achieve a better description of the cross sections, that was the main goal of this work, in order to evaluate the production yields and the contribution to the purity of ^{47}Sc in a more accurate way, as stated in [9]. Therefore, to show the impact of this optimization procedure of the cross sections on the applications in nuclear medicine, another step is required: the evaluation of the production yields of ^{47}Sc and ^{46}Sc , which have been calculated using the new curves and considering the same irradiation conditions identified in [7]. An energy range of the beam of 19-30 MeV, corresponding to a 1.21 mm thick target, has been used in the calculations to maximize the production of ^{47}Sc while minimizing the co-production of ^{46}Sc . In Tab. 2 the estimations of the thick-target yields (TTY) at the end-of-bombardment (EOB) are reported for two irradiation plans of 24 h and 80 h for TALYS modified for the two nuclides in comparison with the values obtained with ISOTOPIA (an online tool developed and maintained by IAEA), which instead seems to underestimate their production, especially for the main contaminant.

Table 2: TTY at EOB for ^{47}Sc and ^{46}Sc for two irradiation time comparing the results obtained with the TALYS modified curve and the ones from ISOTOPIA.

Irradiation time	TALYS modified		ISOTOPIA	
	^{47}Sc	^{46}Sc	^{47}Sc	^{46}Sc
24 h	33.48 MBq/ μA	0.0137 MBq/ μA	25.29 MBq/ μA	0.0013 MBq/ μA
80 h	89.24 MBq/ μA	0.0453 MBq/ μA	67.43 MBq/ μA	0.0042 MBq/ μA

Subsequent steps are represented by the calculation of the radionuclidic purity (RNP) as shown in [6, 29], and dosimetric calculations to assess the dose imparted to the patients.

4 Conclusions

In this work an improvement of the theoretical cross sections for the proton-induced reaction on natural vanadium has been presented working on the nuclear level density parameters of the model based on HF-BCS method implemented inside the TALYS code. In particular the obtained improvements for the case of ^{47}Sc and for its main contaminant, ^{46}Sc , have been shown. The new cross section curve reproduces better the trend of the experimental data, resulting in more accurate and reliable estimations of the production yields to be used for subsequent dosimetric studies, in view of the applications of the theranostic radionuclide.

The tuning procedure is completely general and can also be applied in other studies concerning the production of nuclear medicine radionuclides, as indicated in [6] for the production of ^{47}Sc with proton beams on titanium targets or also in [29] for the production of ^{52}Mn for diagnostic purposes.

References

1. A. R. Jalilian et al., *Curr. Radiopharm.*, **14**, 306-314 (2021), <http://dx.doi.org/10.2174/1874471013999200928162322>
2. C. Müller et al., *Br. J. Radiol.*, **91**, 20180074 (2018), <https://doi.org/10.1259/bjr.20180074>
3. National Nuclear Data Center (NNDC), NuDat 2.8 database, <https://www.nndc.bnl.gov/>, (accessed October 2021)
4. S. Loveless et al., *EJNMMI Res*, **9**, 42 (2019), <https://doi.org/10.1186/s13550-0190515-8>
5. S. M. Qaim, *Medical radionuclide production* (De Gruyter 2019) <https://doi.org/10.1515/9783110604375>
6. F. Barbaro et al., Theoretical study of ^{47}Sc production for theranostic applications using proton beams on enriched titanium targets, (communication at this conference)
7. G. Pupillo et al., *J. Radioanal. Nucl. Chem.*, **322**, 1711-1718 (2019), <https://doi.org/10.1007/s10967-019-06844-8>
8. S. Goriely et al., *Astron. Astrophys.*, **487**, 767-774 (2008), <https://doi.org/10.1051/0004-6361:20078825>
9. F. Barbaro et al., *Phys. Rev. C*, **104**, 04461 (2021), <https://doi.org/10.1103/PhysRevC.104.044619>
10. C. Duchemin et al., *Phys. Med. Biol.*, **60**, 931 (2015), <https://doi.org/10.1088/00319155/60/3/931>
11. A. Colombi et al., *Nucl. Technol.* (2021), <https://doi.org/10.1080/00295450.2021.1947122>
12. F. Minato, *J. Nucl. Sci. Technol.*, **48**, 984-992 (2011), <https://doi.org/10.1080/18811248.2011.9711785>
13. S. Hilaire and S. Goriely, *Nucl. Phys. A*, **779**, 63-81 (2006), <https://doi.org/10.1016/j.nuclphysa.2006.08.014>
14. S. Hilaire et al., *Phys. Rev. C*, **86**, 064317 (2012), <https://doi.org/10.1103/PhysRevC.86.064317>
15. A. Koning et al., *User Manual of Talys-1.9*, (2017), <https://www.talys.eu/>

16. R. Capote et al., Nucl. Data Sheets, **110**, 3107-3214 (2009),
<https://doi.org/10.1016/j.nds.2009.10.004>
17. J. P. Jeukenne et al., Phys. Rev. C, **15**, 10 (1977),
<https://doi.org/10.1103/PhysRevC.15.10>
18. J. P. Jeukenne et al., Phys. Rev. C, **16**, 80 (1977),
<https://doi.org/10.1103/PhysRevC.16.80>
19. F. James and M. Roos, Comput. Phys. Commun., **10**, 343-367 (1975),
[https://doi.org/10.1016/0010-4655\(75\)90039-9](https://doi.org/10.1016/0010-4655(75)90039-9)
20. C. Heiningen and E. O. Wiig, Phys. Rev., **101**, 1074-1076 (1956),
<https://doi.org/10.1103/PhysRev.101.1074>
21. S. Hontzeas and L. Yaffe, Can. J. Chem., **41**, 2194-2209 (1963),
<https://doi.org/10.1139/v63-320>
22. G. Albouy et al., J. Phys., **24**, 67-68 (1963),
<https://doi.org/10.1051/jphysrad:0196300240106700>
23. R. Michel et al., Nucl. Phys. A, **322**, 40-60 (1979),
[https://doi.org/10.1016/03759474\(79\)90332-4](https://doi.org/10.1016/03759474(79)90332-4)
24. R. Michel et al., Nucl. Phys. A, **441**, 617-639 (1985),
[https://doi.org/10.1016/03759474\(85\)90441-5](https://doi.org/10.1016/03759474(85)90441-5)
25. V. N. Levkovskij, (Inter-Vesi: Moscow, Russia, 1991)
26. N. G. Zaitseva et al., Radiochim. Acta, **65**, 157-160 (1994),
<https://doi.org/10.1524/ract.1994.65.3.157>
27. F. Ditrói et al., Nucl. Instrum. Methods Phys. Res. B, **381**, 16-28 (2016),
<https://doi.org/10.1016/j.nimb.2016.05.015>
28. S. M. Grimes et al., Phys. Rev. C., **5**, 85 (1972), <https://doi.org/10.1103/PhysRevC.5.85>
29. M. P. Carante et al., A new route to produce ^{52g}Mn with high purity for MultiModal Imaging, (communication at this conference)